



| | |
|--------------------|--|
| Title | Design and analysis of linear stator permanent magnet vernier machines |
| Author(s) | Du, Y; Chau, KT; Cheng, M; Fan, Y; Wang, Y; Hua, W; Wang, Z |
| Citation | The IEEE International Magnetic Conference (INTERMAG2011), Taipei, Taiwan, 25-29 April 2011. In IEEE Transactions on Magnetics, 2011, v. 47 n. 10, p. 4219-4222 |
| Issued Date | 2011 |
| URL | http://hdl.handle.net/10722/158728 |
| Rights | ©2011 IEEE. Personal use of this material is permitted. However, permission to reprint/republish this material for advertising or promotional purposes or for creating new collective works for resale or redistribution to servers or lists, or to reuse any copyrighted component of this work in other works must be obtained from the IEEE. |

Design and Analysis of Linear Stator Permanent Magnet Vernier Machines

Yi Du^{1,2}, K. T. Chau^{1,3}, Ming Cheng¹, Ying Fan¹, Yubin Wang¹, Wei Hua¹, and Zheng Wang¹

¹School of Electrical Engineering, Southeast University, Nanjing 210096, China

²School of Electrical and Information Engineering, Jiangsu University, Zhenjiang 212013, China

³Department of Electrical and Electronic Engineering, The University of Hong Kong, Hong Kong

This paper presents a new class of linear permanent magnet (PM) vernier machines which is suitable for low speed and high thrust force applications. The machine is composed of a tubular stator and a tubular translator. The stator consists of an iron core with salient teeth wound with 3-phase armature windings and PMs mounted on the surface of stator teeth. The translator is designed as a simple tubular iron core with salient teeth so that it is very robust to transmit high thrust force. By using the finite element method, the characteristics and performances of the proposed machine are analyzed and verified.

Index Terms—High thrust force, linear machine, low speed, stator permanent magnet (PM) machine, vernier machine.

I. INTRODUCTION

LOW speed high thrust force linear machines are more and more attractive for direct-drive applications such as railway traction and wave energy conversion. Compared with the conventional rotary drive system, the linear drive system possesses the merit to eliminate the costly and bulky rotary-to-linear mechanism and the number of energy transformation steps can be reduced. Consequently, the system efficiency can be improved and the system size can be minimized.

In general, the linear machine in the direct-drive system has a bulky size and a large number of poles because of the low-speed operation. Although the use of high energy rare-earth permanent magnets (PMs) has significantly improved the force density of linear machines, a conventional linear PM synchronous machine can only offer about 20–30 kN/m² [1] which is not enough for those low speed, high thrust force applications. Consequently, some special machines have been proposed. In [2], a magnetic gear is artfully integrated with a PM brushless machine to achieve low speed motion and high speed machine design simultaneously. However, it involves three airgaps and two moving parts, thus suffering from the difficulty of manufacture. In [3], the PM vernier machine is developed which employs the magnetic gearing effect. However, it suffers from the problems of mechanical integrity and thermal instability since the PMs are located in the rotor. In [4], the vernier hybrid (VH) machine is proposed which can offer the shear stress of 200–250 kN/m² in theory. In this machine, the PMs are mounted on surface of the stator teeth so that the problems of the mechanical integrity and thermal instability can be avoided. However, the cogging force of this machine is quite large.

The purpose of this paper is to design and analyze a new class of linear stator PM vernier (LSPMV) machines which can produce high thrust force, low speed motion, while exhibiting low cogging force. It should be noted that the LSPMV machine proposed in the paper is a kind of variable reluctance PM machines.

Its translator has salient teeth only without any PMs or windings, and is similar to that of the PM flux switching, switched reluctance and synchronous reluctance machines. However, its stator is fundamentally different from the others, since it incorporates PMs mounted on the stator tooth surfaces. Most importantly, the LSPMV machine makes use of the magnetic gearing principle, based on the relationship between the number of PM poles, the number of armature winding poles and the number of translator teeth, which can significantly reduce the output speed while increase the output force, hence improving the force density. In Section II, the configuration of the proposed machine will be described. In Section III, the machine design will be discussed. In Section IV, the characteristics of the proposed machine will be analyzed by using the finite element method (FEM). Finally, conclusion will be drawn in Section V.

II. MACHINE CONFIGURATION

Fig. 1 shows the configuration of the proposed machine which is composed of a tubular stator and a tubular translator. The stator consists of an iron core with salient teeth wound with 3-phase armature windings and PMs inset on the surface of the stator teeth. The magnetization directions of these PMs are adjacent alternant. Thus the magnet flux in the airgap is almost sinusoidal. The translator is designed as a simple tubular iron core with salient teeth so that it is very robust to transmit high thrust force.

The proposed LSPMV machine operates similarly as the conventional PM vernier machine. The key difference is that the PMs are located in the stator (not in the translator), and the translator teeth function to modulate the magnetic fields produced by the PMs. In order to facilitate the insertion of armature winding, the stator adopts the open slot structure and there is no PM mounted between the adjacent stator teeth. Since this opening does not involve iron core, it will not significantly affect the machine performance. Then each of the stator teeth can be considered as a single vernier construction and the phase of the flux linkage in each of them can be modulated through adjusting the distance between the adjacent stator teeth.

Compared with the existing linear VH (LVH) machine, the number of PMs on each stator tooth of the proposed LSPMV machine is not limited to be an even number. Table I shows a comparison between the existing LVH machine and the proposed LSPMV machine, where p_w is the pole-pair number of

Manuscript received February 20, 2011; accepted May 09, 2011. Date of current version September 23, 2011. Corresponding author: K. T. Chau (e-mail: ktchau@eee.hku.hk).

Color versions of one or more of the figures in this paper are available online at <http://ieeexplore.ieee.org>.

Digital Object Identifier 10.1109/TMAG.2011.2156392

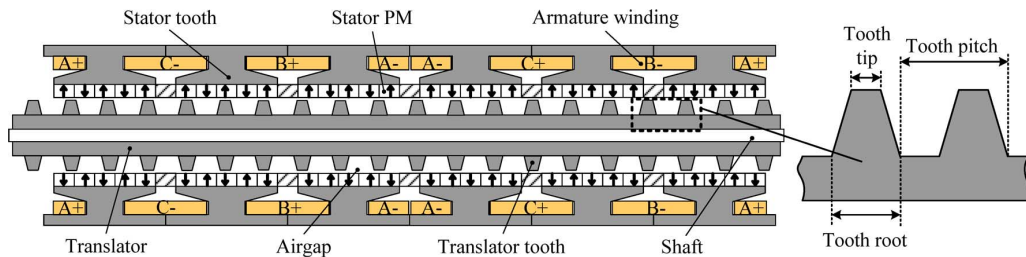


Fig. 1. Proposed LSPMV machine configuration.

TABLE I
COMPARISON BETWEEN LVH AND LSPMV MACHINES

| | n_{pm} | n_s | p_t |
|---------------------------|----------|-------|-------|
| LVH machine | 4 | 6 | 14 |
| | | 12 | 28 |
| | 6 | 6 | 20 |
| | | 12 | 40 |
| LSPMV machine ($p_w=1$) | 4 | 6 | 16 |
| | | 12 | 31 |
| | 5 | 6 | 19 |
| | | 12 | 37 |
| | 6 | 6 | 22 |
| | | 12 | 43 |

armature winding, n_{pm} is the number of the PMs on each stator tooth, n_s is the number of stator teeth, and p_t is the number of active teeth of the translator. It can be found that the least common multiple between the pole-pair number of the PMs and the number of active teeth of the translator of the LSPMV machine is larger than that of the LVH machine. Hence, the cogging force of the proposed machine can be minimized by properly selecting the pole-pair number of PMs and the number of active teeth of the translator.

III. MACHINE DESIGN

A. Operation Principle

According to the principle of magnetic gears [5], the relationship among p_w , p_t and the pole-pair number of PMs p_{PM} of the LSPMV machine is given by

$$p_w = |p_t \pm p_{PM}|. \quad (1)$$

The corresponding linear speed relationship between the translator and the magnetic field in the armature winding produced by the PMs can be expressed as

$$v_{PM} = G_r v_t \quad (2)$$

$$G_r = \frac{p_t}{p_w} \quad (3)$$

where v_t and v_{PM} are the linear speeds of the translator and the magnetic field produced by the PMs in the armature winding, respectively, and G_r is the so-called magnetic gear ratio. Also, the linear speed of the translator can be expressed as

$$v_t = f \tau_t \quad (4)$$

$$\tau_t = l_a / p_t \quad (5)$$

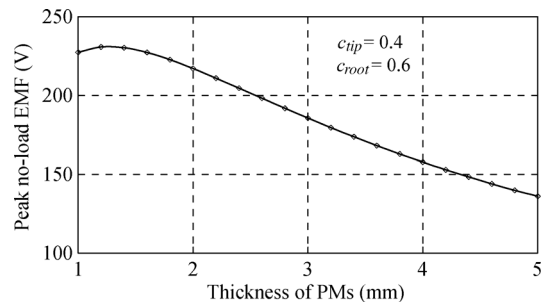


Fig. 2. Peak no-load EMF versus PM thickness.

where f is the frequency of the armature current, τ_t is the tooth pitch of the translator, and l_a is the corresponding active length. The LSPMV machine can achieve low-speed operation because of the fact that p_t is usually designed with a large value.

The magnetic field produced by the armature winding current must have the same pole-pair number and the same linear speed as v_{PM} . It yields

$$v_{PM} = v_i \quad (6)$$

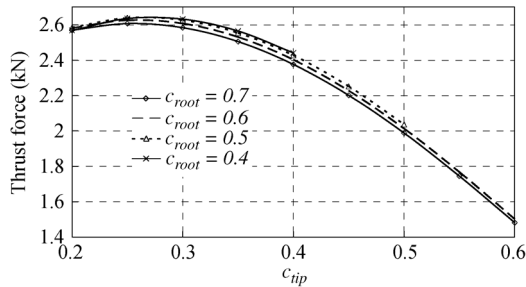
where v_i is the linear speed of the magnetic field produced by the armature winding current. If a proper current is fed to the armature winding, a steady thrust force will be produced. In order to achieve the highest thrust force density, the corresponding magnetic gear ratio should be maximized. Hence, the pole-pair number of armature windings should be selected as unity.

B. Thickness of PMs

The thickness of PMs t_{PM} affects the machine performance significantly. The peak no-load EMF waveform versus the PM thickness is plotted in Fig. 2, where c_{tip} is defined as the ratio of the width of translator tooth tip to the translator tooth pitch, and c_{root} is defined as the ratio of the width of translator tooth root to the translator tooth pitch as shown in Fig. 1. It indicates that the peak no-load EMF can achieve the maximum value when t_{PM} is 1.4 mm. On the other hand, t_{PM} needs to be thick enough to avoid from accidental irreversible demagnetization. Taking into account these two factors, the PM thickness of this machine is designed as 2.6 mm.

C. Width of Translator Teeth

Fig. 3 shows the performance characteristics of the thrust force at different values of c_{tip} and c_{root} . It can be observed that the thrust force achieves the maximum value when c_{tip} and

Fig. 3. Characteristics of thrust force versus c_{tip} at different c_{root} .TABLE II
KEY PARAMETERS OF LSPMV MACHINE

| | |
|--|-----|
| Rated total power (kW) | 2.7 |
| Rated voltage per phase (V) | 150 |
| Rated current (A) | 6 |
| Slot current density (A/mm) | 5 |
| Rated speed (m/s) | 1 |
| No. of PMs on each stator tooth | 5 |
| PM thickness (mm) | 2.6 |
| No. of active translator teeth | 19 |
| Translator tooth height (mm) | 1.1 |
| c_{root} | 0.4 |
| c_{tip} | 0.3 |
| Stator armature winding pole-pair number | 1 |
| Active stator length (mm) | 216 |
| Stator outside diameter (mm) | 272 |
| Stator armature winding per phase (turn) | 220 |
| Airgap length (mm) | 1 |

c_{root} equal 0.3 and 0.4, respectively. Actually, c_{root} does not have a significant effect on the thrust force.

Consequently, a 3-phase 6/2-pole LSPMV machine is designed. The corresponding key parameters are listed in Table II.

IV. FINITE ELEMENT ANALYSIS

The static characteristics of the proposed machine are analyzed by using the FEM. Fig. 4 shows its magnetic field distributions at no-load and full-load. It can be seen that the flux density in the iron core at full-load is much higher than that at no-load. Thus, the machine design process needs to consider the full-load condition.

The radial airgap flux density waveforms due to the PMs are depicted in Fig. 5(a). The corresponding harmonic spectrum is plotted in Fig. 5(b). It can be seen that there are a number of asynchronous space harmonics due to the modulation of the translator teeth, in which the main harmonics include the 1st, 6th, 12th, 18th, and so on. Because of the magnetic gearing effect [6], the 1st harmonic flux travels at the linear speed of 19 times the speed of the translator as governed by $G_r = p_t/p_w = 19$ in (3), whereas the 6th, the 12th and the 18th harmonic flux are produced by the stationary PMs and the speed of the three harmonics equal zero. So, the 1st harmonic is the most effective component for force or power transmission. Other major harmonics, especially the 18th harmonic flux, will inevitably in-

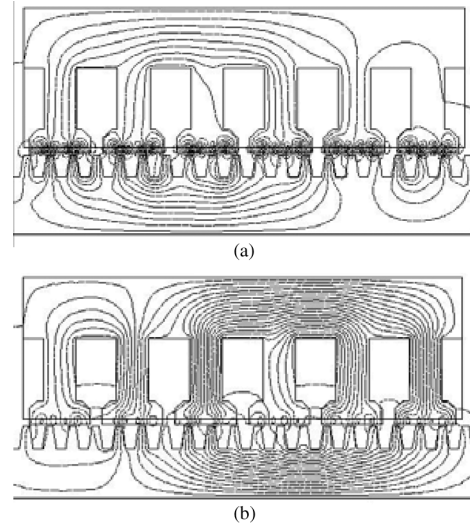


Fig. 4. Flux distributions no-load and full-load. (a) No-load. (b) Full-load.

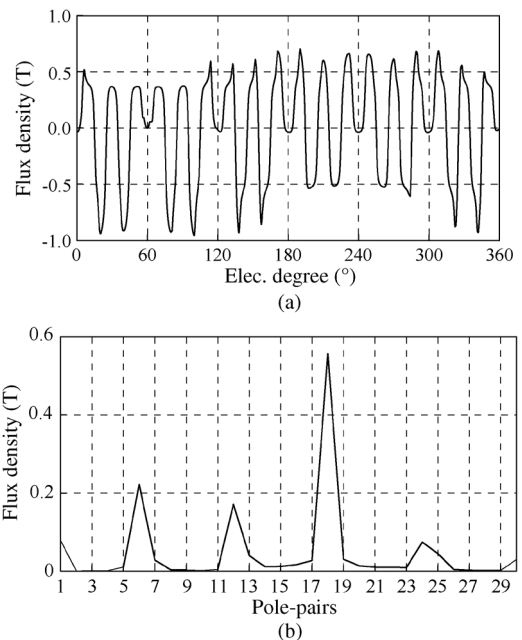


Fig. 5. Flux density in airgap due to PMs. (a) Waveform. (b) Spectrum.

duce the eddy current loss, especially in the translator which needs to be reduced by using the laminated iron core.

Fig. 6 shows the 3-phase flux linkage waveforms which are sinusoidal because those triplen harmonic fluxes, namely the 6th, 12th and 18th, are inherently suppressed by the 3-phase system. Thus, the no-load EMF waveforms are also sinusoidal. The no-load EMF e is given by

$$e = -\frac{d\psi_{PM}}{dt} = -\frac{d\psi_{PM}}{dx}v_t \quad (7)$$

where ψ_{PM} is the flux linkage due to PMs.

The proposed machine can achieve a high no-load EMF even at a low v_t because of the magnetic gearing effect that the linear speed of ψ_{PM} is 19 times the speed of the translator as governed by $G_r = p_t/p_w = 19$ in (3). Fig. 7 shows its 3-phase no-load EMF waveforms at the rated translator speed of 1 m/s, which

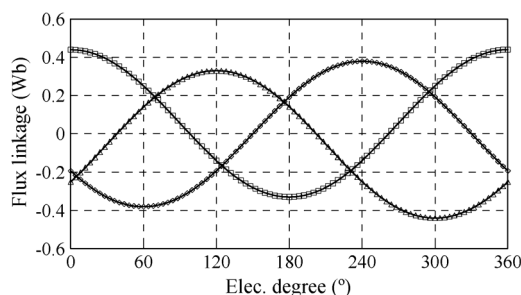


Fig. 6. Flux linkage waveforms.

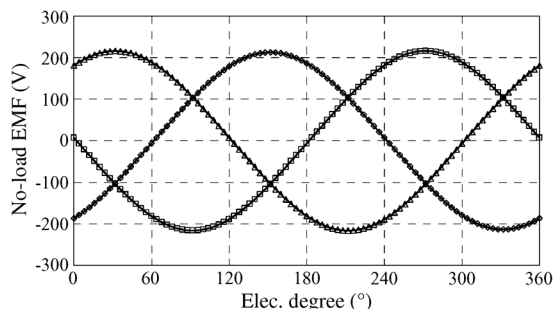


Fig. 7. No-load EMF waveforms

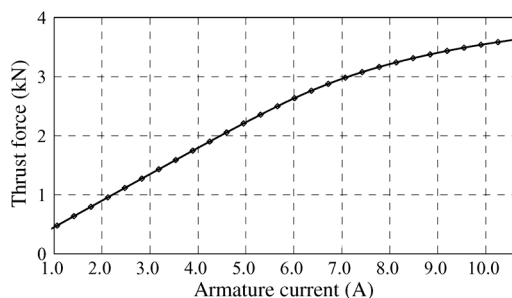


Fig. 8. Current-versus-force characteristic.

confirms that the no-load EMF can achieve the RMS value of 152 V at the translator speed of 1 m/s. The corresponding THD is only 1.4%, which is very acceptable.

Fig. 8 shows the characteristic of armature current versus thrust force of the proposed machine. It can be seen that the thrust force increases linearly with the armature current when it is below the rated value of 6 A, whereas the increase of thrust force is gradually clipped when beyond the rated armature current. It indicates that magnetic saturation occurs at the iron core when the armature current is large.

The rated thrust force waveform is shown in Fig. 9. It can be seen that the average thrust force are 2.6 kN which means that the proposed machine can offer 36 kN/m^2 under the air-cooling condition. The corresponding cogging force is very small as depicted in Fig. 10. It can be seen that the peak-to-peak value of the cogging force is only 13 N which is less than 0.5% of the rated thrust force.

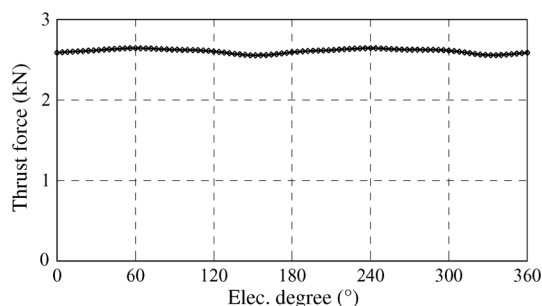


Fig. 9. Rated thrust force waveform.

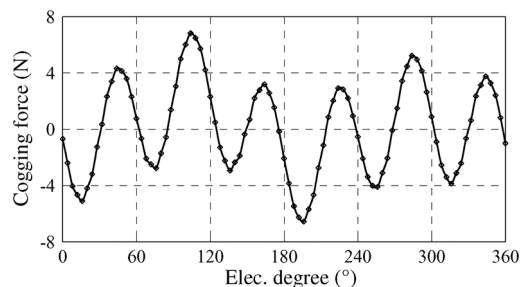


Fig. 10. Cogging force waveform.

V. CONCLUSION

This paper has proposed a new LSPMV machine which is suitable for low speed and high thrust force applications. The machine configuration, operation principle, and design criteria are discussed. Based on the FEM, the static characteristics such as the flux linkage, thrust force and cogging force are analyzed. It confirms that the proposed machine can achieve the desired high thrust force for low speed operation. Also, the machine can offer the advantages of high force density, large no-load EMF and low cogging force.

ACKNOWLEDGMENT

This work was supported and funded in part by grants (Project No. 50729702 and 50907031) from the National Natural Science Foundation of China, a grant from the Chang Jiang Chair Professorship at Southeast University, Nanjing, and a grant from “333 Program” of Jiangsu Province, China.

REFERENCES

- [1] P. R. M. Brooking and M. A. Mueller, *Proc. Inst. Elect. Eng.—Gen., Trans. Distrib.*, vol. 152, no. 5, pp. 673–681, 2005.
- [2] L. Jian, K. T. Chau, and J. Z. Jiang, *IEEE Trans. Ind. Appl.*, vol. 45, no. 3, pp. 954–962, May–Jun. 2009.
- [3] A. Toba and T. A. Lipo, in *Proc. IAS Annu. Meeting*, 1999, pp. 2539–2544.
- [4] E. Spooner and L. Haydock, *Proc. Inst. Elect. Eng.—Electric Power Appl.*, vol. 150, no. 6, pp. 655–662, 2003.
- [5] K. Atallah and D. Howe, *IEEE Trans. Magn.*, vol. 37, no. 4, pt. I, pp. 2844–2846, Jul. 2001.
- [6] L. Jian and K. T. Chau, *IEEE Trans. Energy Convers.*, vol. 25, no. 2, pp. 319–328, Jun. 2010.